

The warm and dense interstellar medium observed with Herschel/HIFI

V. Ossenkopf^{1,2}

M. Gerin³, R. Güsten⁴, F. Boulanger⁵, A. Fuente⁶, Ch. Joblin⁷, Th. Klein⁴, C. Kramer¹, W. Langer⁸, S. Lord⁹, J. Martin-Pintado¹⁰, D. Neufeld¹¹, S. Philipp⁴, M. Röllig¹, M. Spaans¹², J. Stutzki¹, D. Teysier²

¹ 1. Physikalisches Institut der Universität zu Köln; ² SRON, National Institute for Space Research, Groningen; ³ LERMA, Observatoire de Paris; ⁴ MPIFR, Bonn; ⁵ IAS, Université Paris; ⁶ OAN, Madrid; ⁷ CESR, Toulouse; ⁸ JPL, Caltech, Pasadena; ⁹ IPAC, Caltech, Pasadena; ¹⁰ CSIC, Madrid; ¹¹ Johns Hopkins University, Baltimore; ¹² Kapteyn Astronomical Institute, Groningen



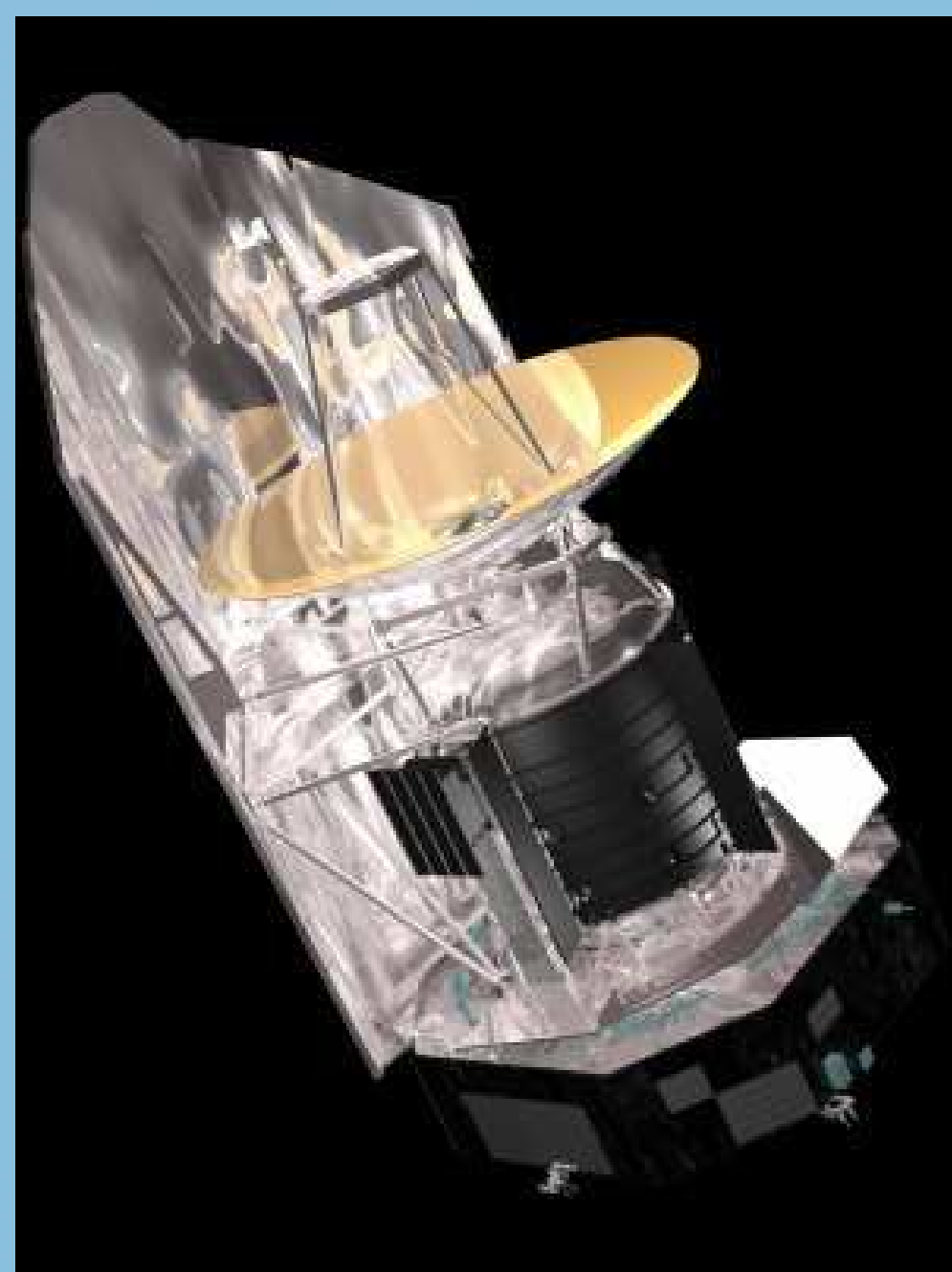
Summary

The combination of HIFI and PACS observations provide a unique way to study the chemical inventory and the energy balance in dense interstellar clouds heated by UV radiation (PDRs) or by shocks from massive stars.

The wide spectral coverage of the instruments allows to observe the key species in the chemical network, like hydrides or H_3O^+ , in their ground states. This will solve many of today's puzzles in the interstellar chemistry. With the spectral resolution of HIFI it will be possible to separate the role of shocks and PDRs, to study the dynamical structure of evaporating molecular clouds, and to resolve the three-dimensional abundance distribution of species. The combination of line and continuum observations will allow to test the available models on the energy balance in the interstellar medium and the systematic observation of many OH and water lines provides a clue to current contradictions in our understanding of the shock water chemistry. The Herschel observations have to be accompanied by ground-based observations for the CI, mid-J CO, and H_2 lines, the sub-mm continuum and other species that can be detected through the atmospheric windows.

The Herschel satellite

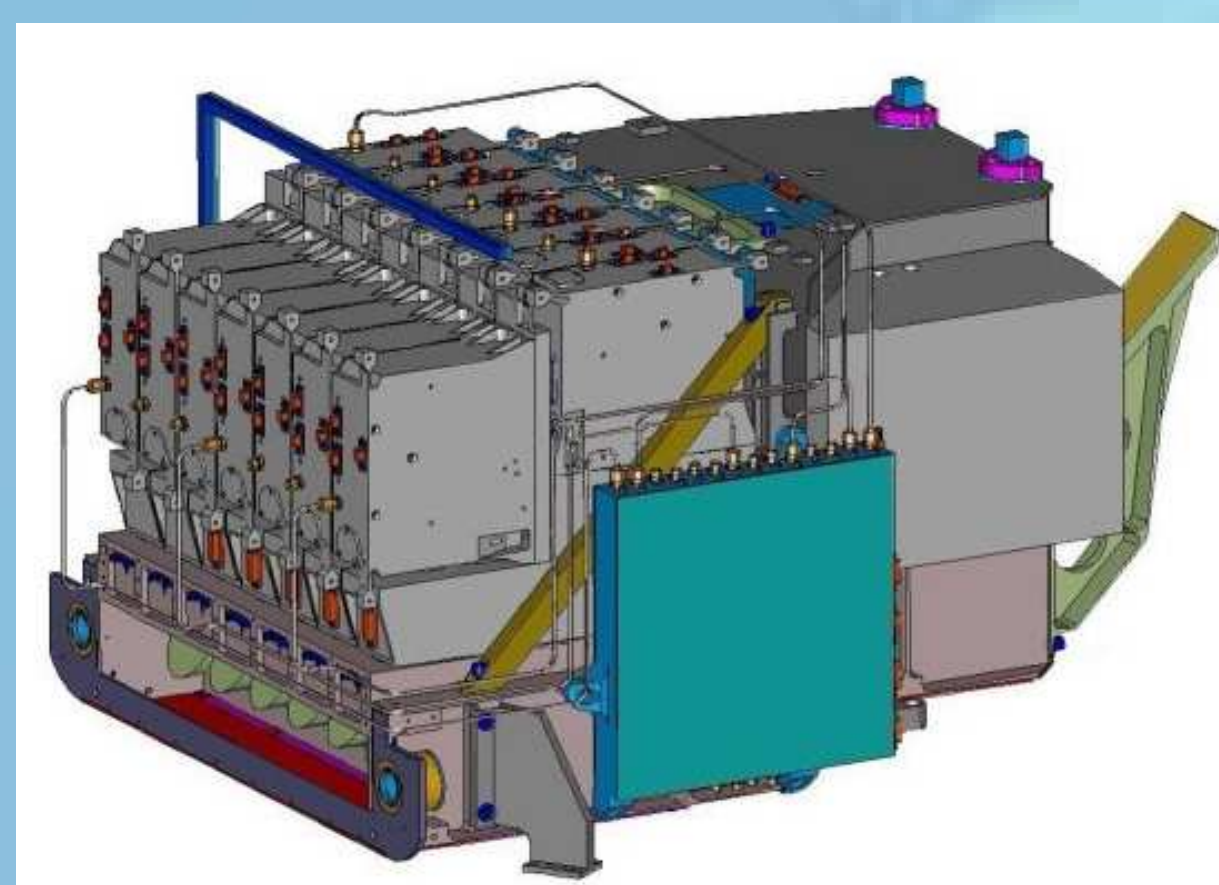
- 3.5m telescope at 80 K
- pointing accuracy < 3.7" (1.5" goal)
- Lissajous orbit in the L2 Lagrange point of the sun-earth system
- launch 2007 with Ariane 5
- operational lifetime > 3 years
- covered wavelength range: 60-670 μm



Instruments:

- **HIFI** (Heterodyne Instrument for the Far-Infrared): 155-620 μm ; 1-pixel dual polarization heterodyne receiver
- **PACS** (Photodetector Array Camera & Spectrometer): 60-210 μm ; 2-band photometer, 64×32 pixels; slit spectrograph, 5×5 pixels, $\lambda/\Delta\lambda = 1700$
- **SPIRE** (Spectral and Photometric Imaging Receiver): 200-500 μm , 3-band photometer, 88-139 pixels; FTS, 19-37 pixels, $\lambda/\Delta\lambda = 20 - 1000$

The HIFI instrument



Schematic drawing of the HIFI focal plane unit

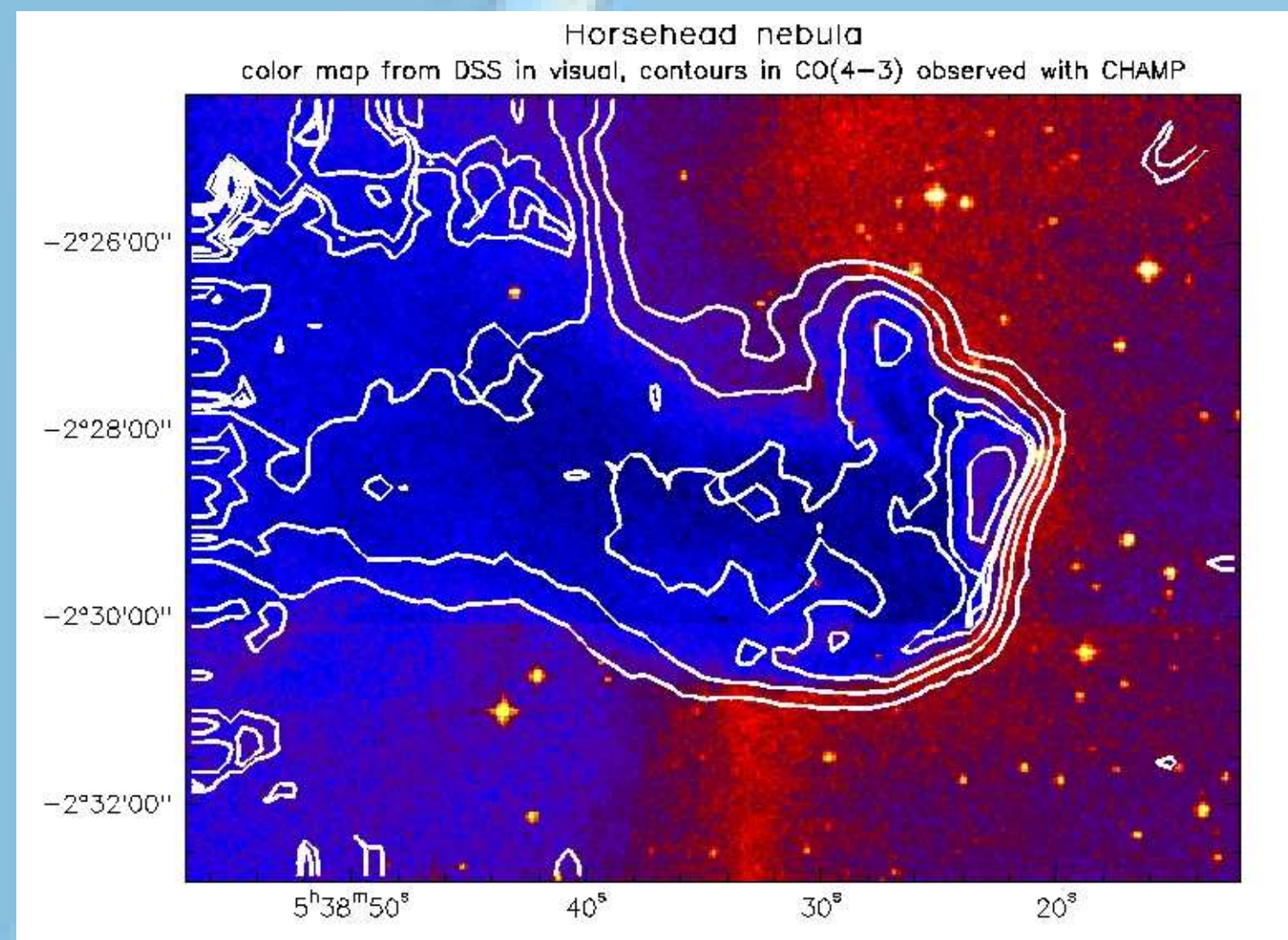
- Continuous frequency coverage 480-1250 GHz and 1410-1910 GHz
- Spectral resolution 130 kHz-1.1 MHz
- Instantaneous bandwidth 4 GHz (2.4 GHz above 1410 GHz)
- Near-quantum noise limit sensitivity ($\approx 3h\nu/k$)
- Two polarizations simultaneously
- Calibration accuracy < 10 % (goal 3 %)

References

- Abergel A., Teysier D., Bernard J. P., et al., 2003, A&A 410, 577
 Bergin, E.A., Melnick, G.J., Stauffer, et al., 2000, ApJ, 539, L129
 Fixsen D.J., Bennett C.L., Mather J.C. 1999, ApJ 526, 207
 Fuente, A.; Rodriguez-Franco, A.; Garcia-Burillo, S.; Martin-Pintado, J.; Black, J. H., 2003, A&A 406, 899
 Gerin M., Viala Y., Pautz F., Ellinger Y., 1992, A&A 266, 463
 Gorti U., Hollenbach D. 2002, ApJ 573, 215
 Habart E., Boulanger F., Verstraete L., et al., 2004, A&A 414, 531
 Hollenbach D.J., Tielens A.G.G.M. 1999, Rev. Mod. Phys. 71, 173
 Kaufman, M.J., Wolfire, M.G., Hollenbach, D.J. & Luhman, M.L., 1999, ApJ, 1999, ApJ, 527, 795
 Kramer C., Stutzki J., Winnewisser G. 1996, A&A 307, 915
 Kramer C., et al. 2004, A&A 424, 887
 Le Bourlot, J., Pineau des Forêts, G., Roueff, E. & Flower, D.R., 1993, A&A, 267, 233
 Liszt H., Lucas R. 2002, A&A 391, 693
 Ossenkopf V., Trojan Ch., Stutzki J. 2001, A&A 378, 608
 Pety J., Teysier D., et al., 2004 A&A in press.
 Schneider N., Simon R., Kramer C., et al., 2003, A&A 406, 915
 Spaans, M. & van Dishoeck, 2001, ApJ, 548, L217
 Sternberg A., Dalgarno A. 1995, ApJS 99, 565
 Störzer, H. & Hollenbach, D.J., 1998, ApJ, 495, 853
 Teysier D., Fossé D., Gerin M., et al. 2004 A&A 417, 135
 Tielens, A.G.G.M. & Hollenbach, D.J., 1999, RvMP, 71, 173
 Wolfire, M.G., Hollenbach, D.J. & Tielens, A.G.G.M., 1993, ApJ, 402, 195

Photon-dominated regions (PDRs)

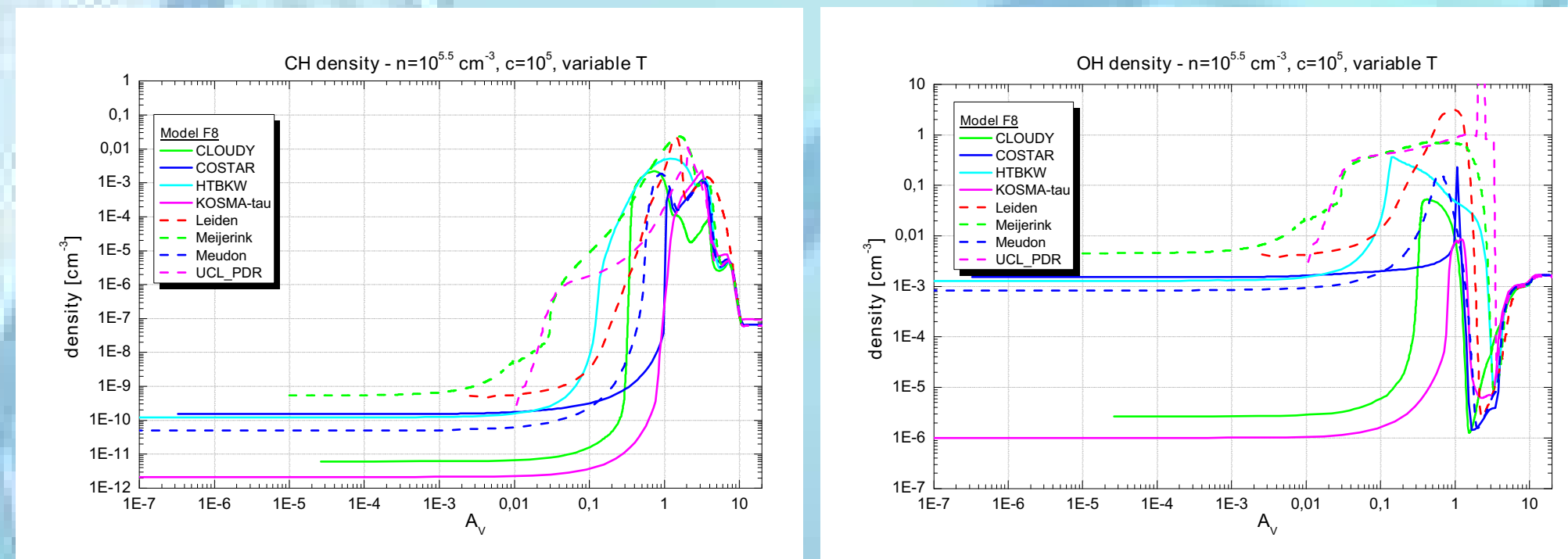
PDRs are transition zones in the interstellar medium between a region of ionized or atomic gas characterized by a low UV optical depth and a region of high-density, typically molecular gas with a large UV optical depth. In PDRs the external radiation field completely determines the thermal and chemical structure of the interstellar gas. As such, PDRs are direct manifestations of the energy balance of interstellar gas and their study allows to understand how the ISM survives the presence of the stars that it forms.



The Horsehead Nebula is a well known example of a PDR. The UV radiation from σ Ori induces a complex chemistry on the surface of the molecular cloud and heats the molecular gas as indicated by the warm CO emission

PDR models

Detailed models of PDRs have been constructed over the past decades. They allow us to determine, with increasing confidence: the density and temperature structure, and the strength of the impinging radiation field. However, basic parts of the interplay between chemistry and dynamics and radiation transfer are still poorly understood. Thus different models predict completely different abundances for key species in the chemical network.



Comparison of the abundance profiles of CH and OH computed from different current PDR models for equal input parameters for a cloud with a density of $10^{5.5} \text{ cm}^{-3}$ and an impinging radiation field of 10^5 times the average Galactic radiation field.

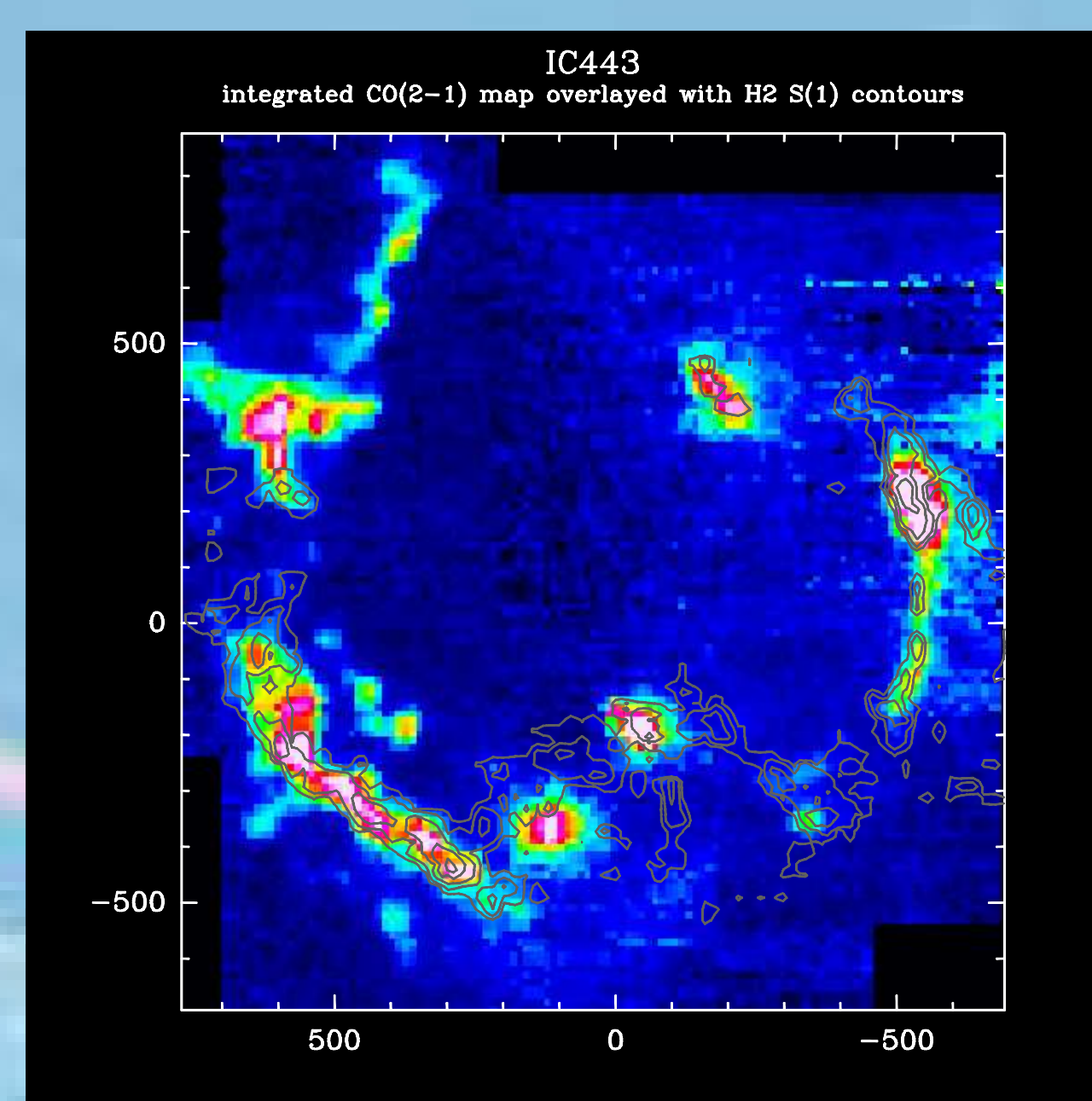
By obtaining a comprehensive inventory of species, containing in particular also the light hydrides representing key nodes in the chemical network, the current models can be tested and revised.

With Herschel it will be possible to:

- Determine the dynamical structure of cloud surfaces
- Obtain an exact measure for the energy balance in PDRs
- Probe the most relevant chemical processes in PDRs
- Investigate the role of the dust properties on the thermal and dynamical properties

Shock regions

Observations of the interaction of blast waves with the surrounding atomic and molecular gas provide an excellent tool to support our theoretical understanding of molecular shocks.



Velocity-integrated emission of CO(2-1), outlining the structure of the molecular gas compressed by the SNR blast wave. Superimposed is the integrated H_2 emission, which nicely traces the interaction layer between the blast wave and the molecular gas.

- In a *jump* (J) shock all the heating occurs in a very small region and the gas subsequently cools in a hot post-shock relaxation layer. Thus J-shocks are mostly dissociative.
- In *continuous* (C) shocks, parameters vary smoothly from pre- to post-shock conditions. Heating occurs in an extended layer where heating and cooling processes compete. The temperature is lower and C-shocks are more non-dissociative.

By directly observing the chemical composition and the main cooling species with HIFI and PACS, the critical information on the state of the shocked gas can be obtained. HIFI's high spectral resolving power will be crucial to provide the kinematic information that is needed to disentangle the emission of the shocked gas from the emission of the quiescent cloud.

Proposed observations

We propose to perform FIR spectroscopy of molecular clouds heated by UV radiation from massive stars, and by the dynamic impact from violent outflows from these stars. Using the high resolution of HIFI we can for the first time simultaneously determine the gas composition and its kinematics in a large set of sources.

HIFI is the ideal instrument to reveal the interplay between dynamics and chemistry in PDRs. Its spectral range covers the frequencies where most of the energy from PDRs is emitted in lines. Its wide frequency coverage allows to observe many species from the complex chemical network in PDRs under similar conditions and its high frequency resolution allows to measure the exact velocity structure of the interstellar material in the observed region. From the details of the line profile we can distinguish between the various emission components along the line-of-sight and within the beam as most profiles will be a composite of contributions from the cool gas inside molecular clouds and the warm gas heated by UV radiation or shocks.

To solve the energy balance problem, the HIFI observations have to be complemented by the observation of lines at higher frequencies by PACS observations.

Herschel observations will aim at the following tracers:

- main cooling species regulating the energy balance
- key species in the chemical network

Line candidates for HIFI observations to trace the chemical and physical structure of PDRs and shocks

molecule	transition	frequency [GHz]	lower level energy [K]	$K_{\text{LTE,rel}}$ [km/s cm ²]		
				at 10 K	at 50 K	at 300 K
CH	$^2P_{3/2} - ^2P_{1/2}$	1900.545	0	$7.5 \cdot 10^{-18}$	$4.8 \cdot 10^{-18}$	$8.0 \cdot 10^{-19}$
CII	$^2\Pi_{3/2} 1, 2^- - ^2\Pi_{1/2} 1, 1^+$	536.761	0	$2.2 \cdot 10^{-14}$	$3.8 \cdot 10^{-15}$	$1.5 \cdot 10^{-16}$
	$^2\Pi_{3/2} 2, 3^- - ^2\Pi_{3/2} 1, 2^+$	1656.961	26	$8.8 \cdot 10^{-15}$	$2.1 \cdot 10^{-14}$	$1.9 \cdot 10^{-15}$
CH ⁺	1-0	835.07	0	$1.2 \cdot 10^{-13}$	$2.4 \cdot 10^{-14}$	$1.0 \cdot 10^{-15}$
	2-1	1669.16	40	$4.3 \cdot 10^{-15}$	$3.1 \cdot 10^{-14}$	$3.3 \cdot 10^{-15}$
NH	$^2\Sigma^- 1, 1/2 - 0, 1/2$	974.479	0	$6.5 \cdot 10^{-14}$	$1.6 \cdot 10^{-14}$	$3.9 \cdot 10^{-16}$
NH ⁺	$^2\Pi_{1/2} 3/2, 5/2, 3^- - 1/2, 3/2, 2$	1012.524	0	$4.7 \cdot 10^{-16}$	$7.2 \cdot 10^{-15}$	$7.5 \cdot 10^{-16}$
NH ₃	$1_0 - 0_0$	572.498	0.5	$1.7 \cdot 10^{-13}$	$1.1 \cdot 10^{-14}$	$1.7 \cdot 10^{-16}$
	$2_1 - 1_1$	1168.452	24	$1.3 \cdot 10^{-14}$	$8.4 \cdot 10^{-15}$	$2.3 \cdot 10^{-16}$
OH ⁺	$^2\Sigma^- 1, 2, 5/2 - 0, 1, 3/2$	971.804	0	$3.2 \cdot 10^{-13}$	$8.1 \cdot 10^{-14}$	$3.6 \cdot 10^{-15}$
H ₃ O ⁺	$1_{1,1} - 1_{0,0}$	1655.814	0	$6.5 \cdot 10^{-14}$	$1.7 \cdot 10^{-14}$	$3.5 \cdot 10^{-16}$
	$0_{0,1} - 1_{0,0}$	984.697	7	$4.1 \cdot 10^{-14}$	$1.5 \cdot 10^{-14}$	$2.8 \cdot 10^{-16}$
p-H ₂ O	$1_{1,1} - 0_{0,0}$	1113.343	0	$4.2 \cdot 10^{-13}$	$8.6 \cdot 10^{-14}$	$1.6 \cdot 10^{-15}$
	$2_{0,2} - 1_{1,1}$	987.927	53	$1.5 \cdot 10^{-15}$	$2.1 \cdot 10^{-14}$	$9.0 \cdot 10^{-16}$
o-H ₂ O	$2_{1,1} - 2_{0,2}$	752.033	101	$3.6 \cdot 10^{-17}$	$1.9 \cdot 10^{-14}$	$1.6 \cdot 10^{-15}$
	$1_{1,0} - 1_{0,1}$	556.936	0	$1.9 \cdot 10^{-13}$	$4.2 \cdot 10^{-14}$	$1.1 \cdot 10^{-15}$
	$2_{1,2} - 1_{0,1}$	1669.905	0	$2.0 \cdot 10^{-13}$	$8.0 \cdot 10^{-14}$	$3.0 \cdot 10^{-15}$
	$3_{0,3} - 2_{1,2}$	1716.770	114	$7.7 \cdot 10^{-17}$	$1.9 \cdot 10^{-14}$	$2.8 \cdot 10^{-15}$
HDO	$1_{1,1} - 0_{0,0}$	893.639	0	$2.7 \cdot 10^{-13}$	$2.1 \cdot 10^{-14}$	$3.4 \cdot 10^{-16}$
H ₂ ¹⁸ O	$1_{1,1} - 0_{0,0}$	1101.698	0	$4.2 \cdot 10^{-13}$	$8.5 \cdot 10^{-14}$	$1.6 \cdot 10^{-15}$
OH	$2\Pi_{1/2} 3/2 - 1/2$	1834.747	181	$6.5 \cdot 10^{-22}$	$9.6 \cdot 10^{-16}$	$1.5 \cdot 10^{-15}$
CO	10-9	1151.985	249	$5.8 \cdot 10^{-26}$	$3.7 \cdot 10^{-18}$	$1.0 \cdot 10^{-17}$
	16-15	1841.345	663	$3.2 \cdot 10^{-32}$	$1.8 \cdot 10^{-21}$	$5.9 \cdot 10^{-18}$
¹³ CO	10-9	1101.350	238	$1.7 \cdot 10^{-25}$	$4.3 \cdot 10^{-18}$	$9.6 \cdot 10^{-18}$
	15-14	1650.768	555	$7.5 \cdot 10^{-31}$	$1.4 \cdot 10^{-20}$	$7.0 \cdot 10^{-18}$

Lines candidates for corresponding PACS observations

molecule	transition	wavelength [μm]	lower level energy [K]	$K_{\text{LTE,rel}}$ [km/s cm ²]		
				at 10 K	at 50 K	at 300 K
OH	$^2\Pi_{3/2} 5/2, 1^+ - 3/2, 1^-$	119.44	0	$6.9 \cdot 10^{-14}$	$5.4 \cdot 10^{-14}$	$4.5 \cdot 10^{-15}$
	$^2\Pi_{3/2} 5/2, 1^- - 3/2, 1^+$	119.23	0.1	$6.6 \cdot 10^{-14}$	$5.2 \cdot 10^{-14}$	$4.3 \cdot 10^{-15}$
O	$^3P_1 - ^3P_2$	63.17	0	$5.4 \cdot 10^{-18}$	$5.3 \cdot 10^{-18}$	$2.1 \cdot 10^{-18}$
	$^3P_1 - ^3P_1$	145.53	228	$5.5 \cdot 10^{-28}$	$3.9 \cdot 10^{-20}$	$4.2 \cdot 10^{-18}$

Source candidates

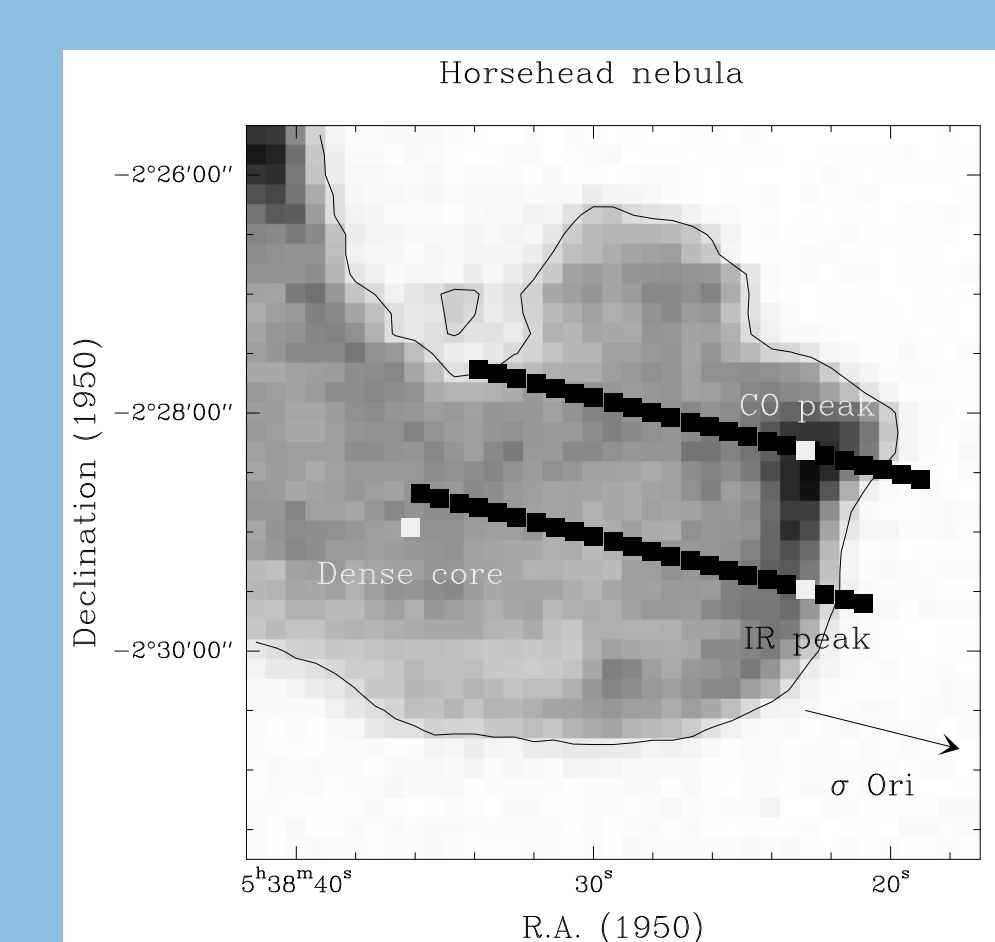
The sources to be observed should:

- cover a wide range of cloud properties, i.e. density (10^3 to 10^7 cm^{-3}), radiation field (1 to 10^5 average Galactic radiation fields), shock velocity, dust properties, and properties of the ionization front.
- be located nearby in order to probe small linear scales.
- have a well defined orientation with respect to the observer so that it is possible to analyze the stratified structure of the interface region.
- have a simple geometry with respect to the configuration between the illuminating stars and outflow sources and the molecular cloud.

Observing strategy

To trace the change of the chemical and dynamical structure across the PDR/shock interface, the interface has to be mapped. Different tracers will show different peak emission positions. The observations have to combine two strategies:

- cuts across the interfaces of PDRs and shock regions
- deep integrations at selected positions for rare species



Positions aimed at being observed in the Horsehead nebula, overlaid over an integrated CO(3-2) map. White squares indicate the three positions to be probed in deep integrations, while the black squares indicate the position of the two cuts. The arrow shows the direction of the illuminating star σ Ori.

Complementary observations

Complementary ground-based observational data are needed to complete the wavelength coverage of the physical and chemical processes: H_2 rovibrational lines, the cold dust emission from the shielded cloud interior, and rotational lines of CO, and other "heavy" molecules. The observation of additional molecular species is required to derive the comprehensive inventory of the chemical network.